Int. J. Multiphase Flow Vol. 19, No. 1, pp. 1–13, 1993
Printed in Great Britain.

0301-9322/93 $6.00 + 0.00

TWO-PHASE MIXTURE LEVEL SWELL IN VERTICAL PIPES

T. UEDA and Y. KOIZUMI
Department of Mechanical Engineering, Kogakuin University, 24-2, Nishi-shinjuku 1, Shinjuku-ku, Tokyo 160, Japan

(Received 17 June 1991; in revised form 26 October 1992)

Abstract—The behavior of the two-phase mixture level was examined in the case of bubbling of a stagnant liquid column in vertical pipes and also in the case of bubbling of a liquid column to which liquid is supplied as a falling film. In a range of low air flow rates where the flow pattern is of bubbly type, the mixture level swell and its fluctuation amplitude were small. However, these values increased sharply as the air flow rate was increased and the flow pattern turned into a slug type. The mean height of the two-phase mixture level and the level fluctuation amplitude were analyzed physically and compared with the experimental results.

Key Words: mixture level swell, stagnant liquid column bubbling, bubbling with a falling liquid film, bubbly flow, slug flow, mean level height, level fluctuation amplitude

1. INTRODUCTION

When gas is injected into a stagnant liquid column or boiling occurs in a pool of liquid, the liquid level swells. The swell height of the two-phase mixture plays an important role in some heat and mass transfer processes utilizing bubbling or pool boiling. The fluctuation of the two-phase mixture level is relatively small in systems with a large surface area, such as boiler drums or chemical reactors, since the gas phase is usually dispersed as discrete bubbles in the liquid phase (Wilson *et al.* 1962). However, in the case of bubbling or boiling in a pipe with a small cross section, slug or annular flow appears as the gas flow rate is increased and the mixture level rises higher and fluctuates in a complicated way.

The countercurrent two-phase flow in a vertical open pipe with a falling liquid film is normally of annular type. It has been known that when increasing the gas flow rate flowing upwards in the core of the pipe, a point is reached where a part of the liquid begins to reverse in the upward direction (often defined as flooding). However, when a two-phase mixture exists in the lower portion of the pipe, the liquid behavior seems to be different from the flooding phenomena encountered in open systems. The mixture level swell thus becomes a serious problem in a core or in steam generator U-tubes during a loss-of-coolant accident in a nuclear reactor (Cunningham & Yeh 1973). Similar flow conditions are also observed in closed two-phase thermosiphons. It has been pointed out that the behavior of the two-phase mixture level is closely related to the performance limit of the thermosiphons (Ueda & Miyashita 1990).

In this study, the static and dynamic behavior of the two-phase mixture level are examined in the case where gas is injected into a stagnant liquid column in a vertical pipe, and also in the case where gas is injected into a liquid column with a falling liquid film. In this paper, the former case is referred to as the stagnant liquid column bubbling and the latter case as the countercurrent flow liquid column bubbling.

2. EXPERIMENTAL APPARATUS AND PROCEDURES

The experimental apparatus used in the present study is shown schematically in figure 1. It consists of a vertical pipe, an air supply system connected to the lower end of the test pipe and a water circulation system which supplies water to an upper plenum to initiate a falling water film flow. In the experiments for the stagnant liquid column bubbling, the water circulation system was isolated by closing a valve at the inlet of the water storage tank.

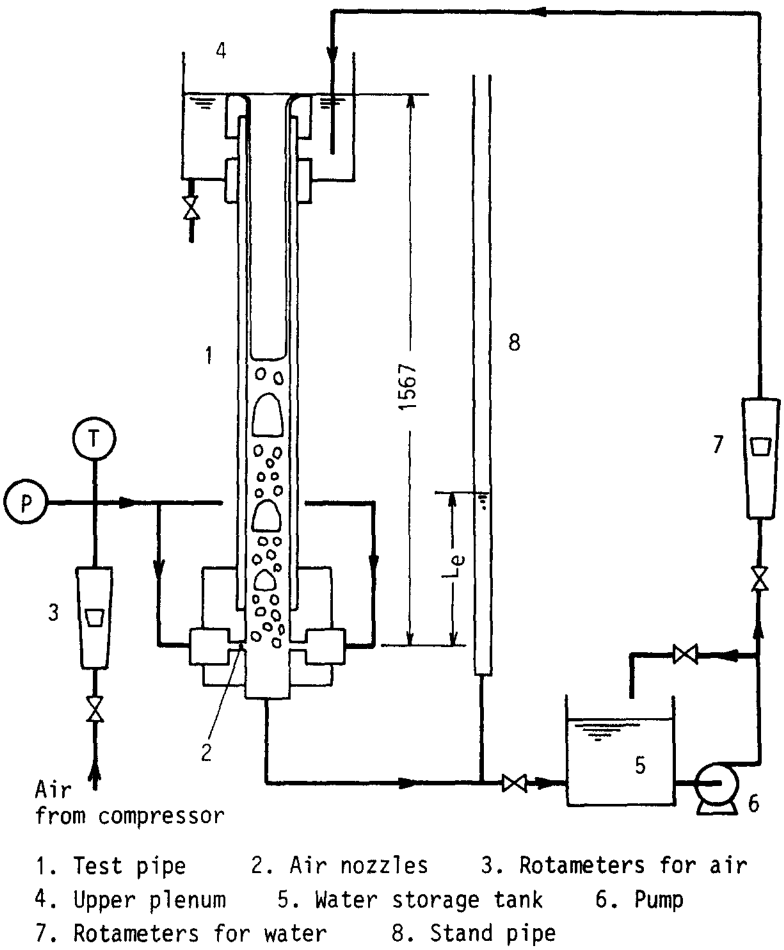

Figure 1. Schematic of the experimental apparatus.

Four Pyrex glass pipes of 1.5 m length were used for the test pipe. The inner diameters of these pipes were $D = 10.0$, 14.8, 20.2 and 26.0 mm, respectively. Air was injected into the test pipe through 12 nozzles of 2 mm dia drilled circumferentially at the lower end of the test pipe. Experiments were conducted with air and deionized water. The height of the bubbling two-phase mixture in the test pipe was measured visually, under the conditions of the water column height in the stand pipe, L_e, being maintained at 60, 120, 240 and 360 mm, respectively.

The experiments for the stagnant liquid column bubbling were conducted in a range of air superficial velocities, U_G, up to 9 m/s. On the other hand, the experiments for the countercurrent flow liquid column bubbling were conducted in a range of U_G up to 4 m/s with the superficial velocities of the falling water, U_{fL}, from 0.01 to 0.095 m/s.

3. EXPERIMENTAL RESULTS

In both the stagnant liquid column bubbling and the countercurrent flow liquid column bubbling, the two-phase mixture level swelled and was accompanied by periodic fluctuations with increasing air flow rate. The maximum and minimum heights of the fluctuating mixture level, L_{max} and L_{min}, were measured. The mean height of the two-phase mixture level, L_m, and the fluctuation amplitude of the level, ΔL, were calculated by

$$L_m = \frac{L_{max} + L_{min}}{2} \qquad [1a]$$

and

$$\Delta L = \frac{L_{max} - L_{min}}{2}. \qquad [1b]$$

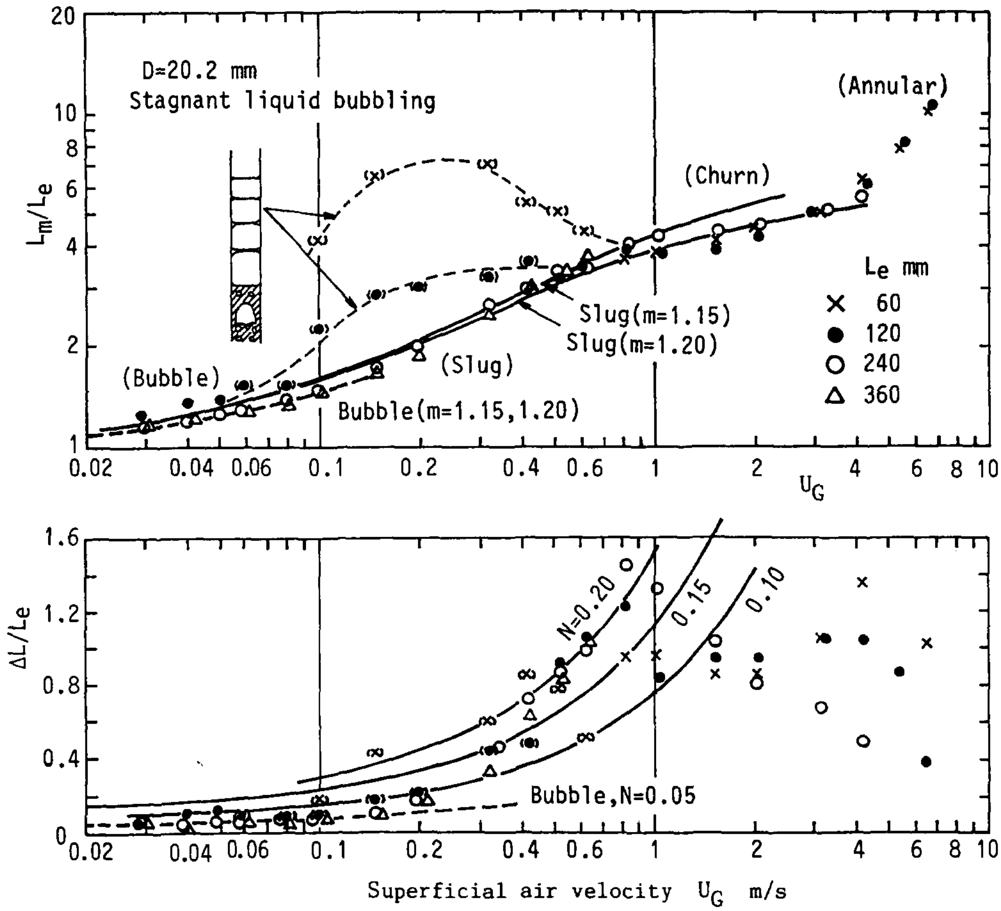

Figure 2. Two-phase mixture level swell and level fluctuation amplitude (stagnant liquid column bubbling, $D = 20.2$ mm).

The ratios of these values to the water column height L_e (i.e. L_m/L_e and $\Delta L/L_e$) were examined in this study. It should be noted here that L_{max} and L_{min} are the mean values of the observed maximum and minimum heights of the fluctuating level, respectively.

The values of L_m/L_e and $\Delta L/L_e$ for the stagnant liquid column bubbling in a pipe of $D = 20.2$ mm are shown in figure 2. The flow pattern was of bubbly type at lower U_G. As U_G was increased, the flow pattern changed to a slug type, a churn (semi-annular) type and then an annular type. Both L_m/L_e and $\Delta L/L_e$ are small in a range of the bubbly flow. The value of L_m/L_e increases with an increase in U_G and then increases sharply as the flow pattern turns into the annular type. The value of $\Delta L/L_e$ increases with an increase in U_G in the slug flow region. However, it tends to decrease and takes random values as the flow pattern turns into the churn type. In this study, the effect of pipe diameter was examined. Both L_m/L_e and $\Delta L/L_e$ showed a tendency to decrease slightly with an increase in the pipe diameter, as will be described later.

In the case of smaller pipe diameters with a small fluctuation in the two-phase mixture level, i.e. at lower L_e, thin water films, like bamboo joints, which bridge the cross section of the pipe were observed. The symbols in parentheses in figure 2 indicate the values for the highest thin film. The rise height for which the thin film disappears was unsteady and the volume of the thin film was small, so the physical importance of the thin film seemed to be limited. Thus, the thin films (data in parentheses) were not considered in the following analyses. When U_G was increased so as to cause droplet entrainment from the mixture interface, the thin films were disrupted. In the countercurrent flow liquid column bubbling, the thin films were hardly observed.

The values of L_m/L_e and $\Delta L/L_e$ for the countercurrent flow liquid column bubbling are shown in figure 3. Both values in the range of the slug flow are larger than those in the stagnant liquid column bubbling. The differences showed a tendency to become larger as the flow rate of the falling water film, i.e. U_{fL}, increased.

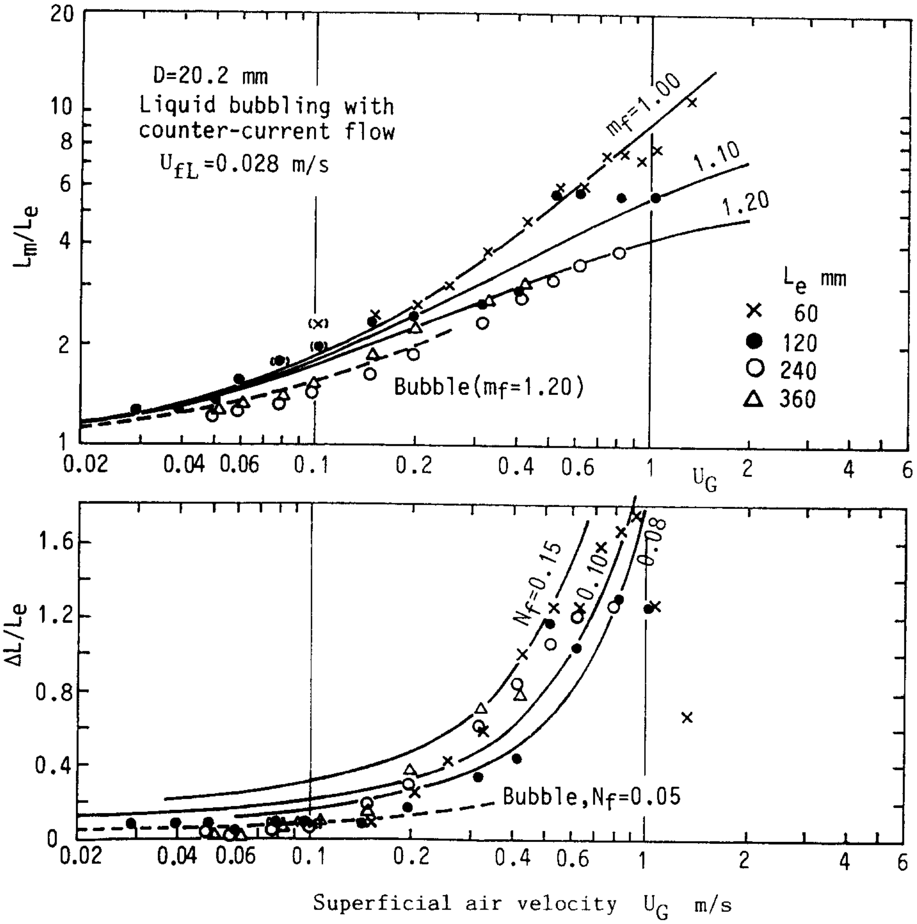

Figure 3. Two-phase mixture level swell and level fluctuation amplitude (countercurrent flow liquid column bubbling, $D = 20.2$ mm and $U_{fL} = 0.028$ m/s).

In this experimental range, the flow pattern of the mixture in the air injection region was always of bubbly type. The bubbles injected through the air nozzles coalesced as they flowed upwards, and large bubbles or gas plugs were formed. When the superficial velocity of air was higher, the bubble coalescence progressed rapidly and slug-type flow prevailed in the upper portion of the mixture. In this paper, the term of the slug or churn flow indicates that the slug or churn type prevails over most of the mixture length.

The effects of the size and number of air nozzles on the mixture level swell were also examined. An example of the results on the mean height of the mixture level is shown in figure 4. When nozzles of 2 mm dia were used, thin water films, like bamboo joints, were observed in the upper portion of the mixture. However, the thin films disappeared as the diameter of the nozzles decreased, as is seen in figure 4.

It seems that the size and number of air nozzles affect the initial bubble size and the bubble coalescence process. Thus, there may be some change in the mixture level swell due to the air nozzle conditions. However, figure 4 suggests that the effects of the nozzle size and number on L_m/L_e are small in the case where no thin film is generated, although some data scattering is noticed in the figure. Experimental results showed that the nozzle size and number also had little effect on $\Delta L/L_e$.

4. ANALYSES

The level swell caused by air injection into the water column is due to void formation in the water column. Relations between the flow rate(s) of the injected air (and the falling water film) and the mean height of the mixture level and the level fluctuation amplitude are analyzed physically for both the stagnant liquid column bubbling and the countercurrent flow liquid column bubbling.

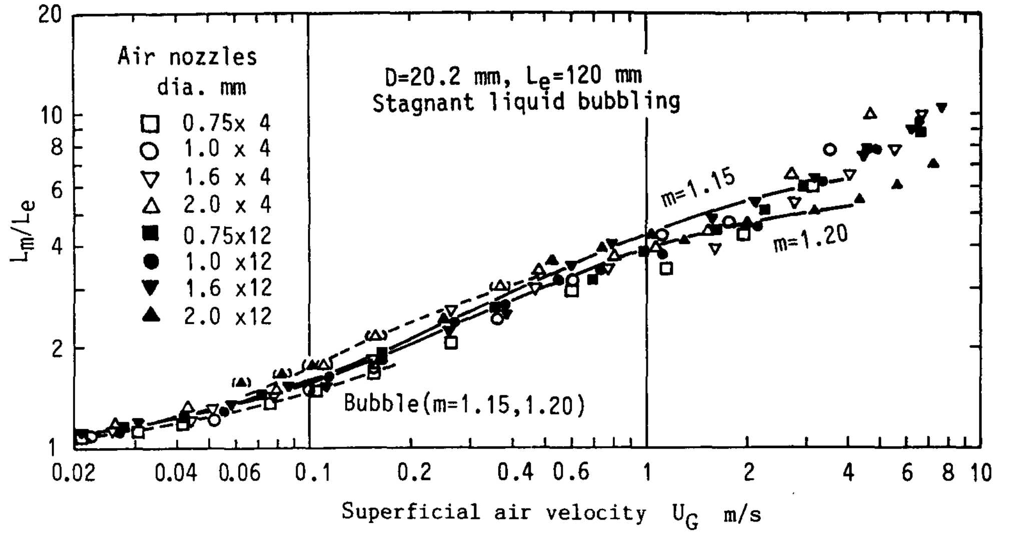

Figure 4. Effect of the air injection nozzles on the two-phase mixture level swell.

4.1. Level swell of the two-phase mixture in the stagnant liquid column bubbling

(1) Description of the physical model. The flow state is assumed to be of slug type, as shown in figure 5. Since the wall shear stress is small, it can be expressed as $L_e \rho_L = L_m \rho_L (1 - \epsilon)$. Thus,

$$\frac{L_m}{L_e} = \frac{1}{1-\epsilon}, \tag{2}$$

where ϵ is the void fraction. The mean velocity of the water between air plugs is equal to U_G, as is obvious from the continuity law. Since water falls down around the air plug as the air plug rises up, the velocity profile of the water in this cross section may take a form such as that shown in figure 5. Assuming that the water velocity in the center portion of the pipe is mU_G and that the air plug has a relative velocity to it (Griffith & Wallis 1961; Nicklin *et al.* 1962), the rise velocity of the air plug, i.e. u_G, can be expressed as

$$u_G = mU_G + c_s\sqrt{gD}. \tag{3}$$

In this equation, the relative velocity is regarded as $c_s(gD)^{1/2}$; the rise velocity of a single plug in stagnant liquid. The value of c_s for such a low viscosity liquid as water is a function of $E_o = \rho_L g D^2/\sigma$

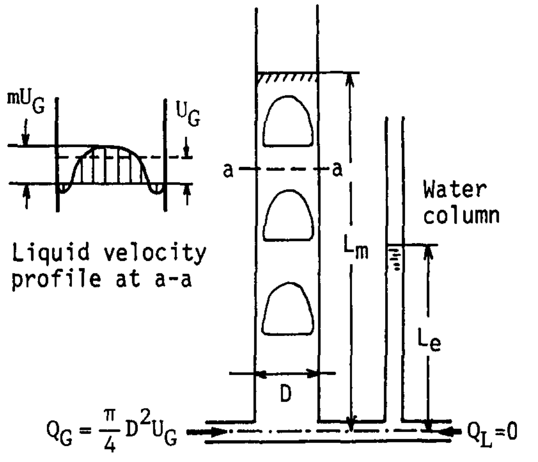

Figure 5. Two-phase mixture level swell by air injection into a stagnant water column.

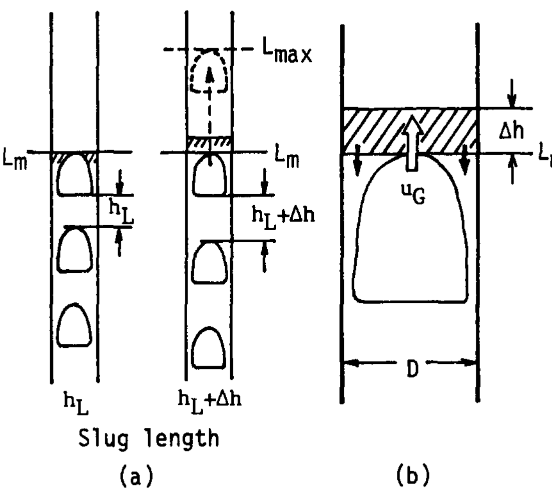

Figure 6. Fluctuation of the two-phase mixture level by air injection into a stagnant water column.

and is equal to 0.35 for $E_o \geqslant 100$ (White & Beardmore 1962). Since the void fraction ϵ is expressed as

$$\epsilon = \frac{U_G}{u_G} = \frac{1}{m + \dfrac{c_s\sqrt{gD}}{U_G}}, \qquad [4]$$

the following equation is derived from [2]:

$$\frac{L_m}{L_e} = \frac{mU_G + c_s\sqrt{gD}}{(m-1)U_G + c_s\sqrt{gD}}. \qquad [5]$$

Next, the fluctuation amplitude ΔL of the two-phase mixture level will be examined. It has been pointed out that the length of the liquid slug is stochastically distributed within a certain range (Akagawa *et al.* 1970). The variation of the liquid slug length is considered to result in the fluctuation of the level around its mean height given by [5].

Assuming the length of the liquid slug to be within $h_L \pm \Delta h$, the mixture level is considered to reach the mean height L_m when the length of the liquid slug is equal to h_L, and reach L_{max} (L_{min}) when the length of the liquid slug is equal to $h_L + \Delta h (h_L - \Delta h)$. Figure 6(a) illustrates the states when the lengths of the liquid slug are h_L and $h_L + \Delta h$. Figure 6(b) shows the state when the top of the air plug which was associated with the liquid slug of $h_L + \Delta h$ on it has just reached the elevation of the mean height L_m. At this moment, the liquid slug of thickness Δh is still left on the air plug.

Although the water ahead of the air plug tip moves up with the same velocity as that of the air plug, i.e. $u_G = mU_G + c_s(gD)^{1/2}$, the air plug has a relative velocity of $c_s(gD)^{1/2}$ to the liquid slug. Therefore, part of the water falls down around the air plug. When the mean void fraction of the air plug is ϵ_{pm}, the volumetric flow rate of the water which falls down around the air plug is expressed as $(\pi/4)D^2\epsilon_{pm}c_s(gD)^{1/2}$.

The liquid slug of thickness Δh at the elevation L_m rises up further and is accompanied by a continuous decrease in its volume. Then, it reaches L_{max} to disappear ($\Delta h = 0$) after Δt_0. Thus, the mass balance for the liquid slug during Δt_0 is given by

$$\frac{\pi}{4}D^2\,\Delta h - \frac{\pi}{4}D^2\epsilon_{pm}c_s\sqrt{gD}\,\Delta t_0 = 0. \qquad [6]$$

From [6], the rise height of the mixture level during this period, i.e. $\Delta L = L_{max} - L_m$, and the ratio $\Delta L/L_e$ are then expressed as follows:

$$\Delta L = u_G\,\Delta t_0 = \Delta h\,\frac{mU_G + c_s\sqrt{gD}}{\epsilon_{pm}c_s\sqrt{gD}} \qquad [7]$$

and

$$\frac{\Delta L}{L_e} = N\left(\frac{U_G}{c_s\sqrt{gD}} + \frac{1}{m}\right). \qquad [8]$$

where

$$N = \frac{\Delta h}{L_e}\cdot\frac{m}{\epsilon_{pm}}.$$

The void fraction ϵ_{pm} in the above equations is determined by the ratio of the length of the air plug to the pipe diameter (Ueda 1981). This value is usually in the range 0.70–0.85. Therefore, provided Δh is proportional to the stagnant water column height L_e, N will be nearly a constant value. The variation in the liquid slug length Δh is caused by the random coalescence of bubbles and gas plugs. The coalescence progresses continuously along the mixture length. This seems to be the reason why the observed value of Δh shows a tendency to increase with increasing L_e.

In the case of bubbly flow, L_m/L_e and $\Delta L/L_e$ may be expressed by applying the relative velocity of a bubble in place of $c_s(gD)^{1/2}$ in [5] and [8]. The present analytical model is for the slug flow and Δh is not well-defined for the bubbly flow. However, the bubble agglomeration and the coalescence to larger bubbles progress at random along the mixture length even in bubbly flow. Therefore, the level fluctuation in bubbly flow seems to occur to some extent in a similar manner to that in slug flow.

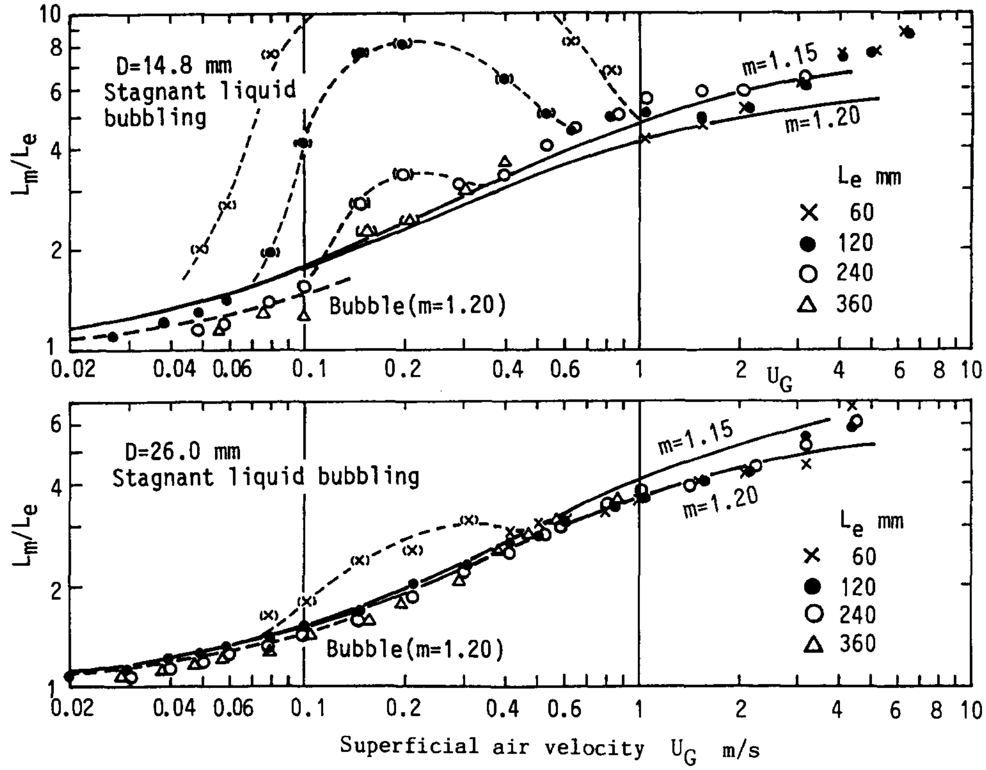

Figure 7. Mean height of the two-phase mixture level (stagnant liquid column bubbling).

(2) Comparison with the experimental results. The ratios of L_m/L_e calculated with [5] are compared with the experimental results in figures 2, 4 and 7. In this calculation, the following approximate equations were used to obtain c_s:

$$\left.\begin{array}{ll} c_s = 0.37 - 1.85/E_0 & \text{for } E_o < 92.5, \\ c_s = 0.35 & \text{for } E_o \geqslant 92.5. \end{array}\right\} \qquad [9]$$

These equations are valid for $E_o \geqslant 7$ (Ueda & Miyashita 1990).

The calculated values for

$$m = 1.15 \text{ to } 1.20 \qquad [10]$$

are in good agreement with the experimental results in the complete range of slug and churn flow.

The dashed lines in figure 7 indicate bubbly flow. In the calculation for bubbly flow, the following equation (Peebles & Garber 1953) was used for the relative velocity in place of $c_s(gD)^{1/2}$ in [5]:

$$u_b = 1.18\left[\frac{\sigma(\rho_L - \rho_G)g}{\rho_L^2}\right]^{1/4}. \qquad [11]$$

The calculated results reproduce the experimental results well. Since U_G is small in the bubbly flow, the calculated results for $m = 1.15$ and 1.20 fall on almost the same line.

The values of $\Delta L/L_e$ calculated with [8] are compared with the experimental results in figures 2 and 8. In this calculation, a mean value of $m = 1.175$ was used. Although the experimental data are somewhat scattered, the data in the slug flow region are close to the values calculated with [8] in which $N = 0.15$ on average. Almost all the data are in a range of the values calculated by

$$N = 0.10 \text{ to } 0.20. \qquad [12]$$

The result suggests that $\Delta h/L_e$ is about one-tenth. This is fairly consistent with the experimental observations for slug flow.

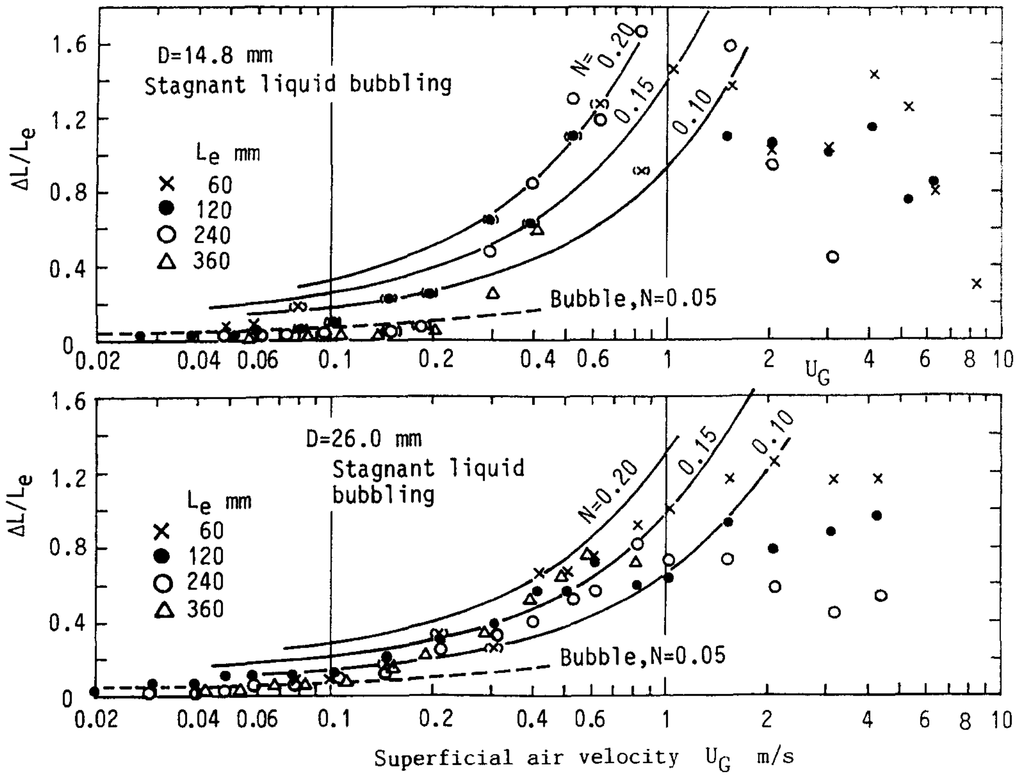

Figure 8. Fluctuation amplitude of the two-phase mixture level (stagnant liquid column bubbling).

Since bubbles are rather uniformly distributed in the mixture, the values of $\Delta L/L_e$ and N should be small for bubbly flow. As is seen in figure 8, the values calculated by

$$N = 0.05 \qquad [12']$$

and using [11] instead of $c_s(gD)^{1/2}$ are in good agreement with the experimental data. This result shows that $\Delta h/L_e$ is smaller and decreases as the void fraction decreases.

Visual observations indicated that the flow pattern was of bubbly type throughout the mixture length up to $\epsilon \fallingdotseq 0.20$ (i.e. $L_m/L_e \fallingdotseq 1.25$). An air plug appeared in the upper portion of the mixture as the void fraction exceeded this value. However, the mixture level swell is affected by the flow state over the whole length of the mixture. Therefore, the transition of the characteristics in the mean level height from bubbly to slug type occurs in the range

$$\epsilon = 0.35 \text{ to } 0.45 \quad (L_m/L_e = 1.5 \text{ to } 1.8). \qquad [13]$$

The value of $\Delta L/L_e$ in the slug flow region increases with an increase in U_G and reaches a maximum value at

$$\epsilon \fallingdotseq 0.78 \quad (L_m/L_e \fallingdotseq 4.5). \qquad [14]$$

The maximum values of $\Delta L/L_e$ are in the range 1.0–1.5. The value of U_G at the point where $\Delta L/L_e$ reaches a maximum increases with an increase in the pipe diameter. After U_G exceeds this value, the flow pattern changes to a churn type, L_m/L_e increases gradually and $\Delta L/L_e$ begins to decrease. With a further increase in U_G, the flow pattern finally turns into an annular type. In the present experiments, the transition to annular flow occurred in the following range of nondimensional air superficial velocities:

$$j_G^* = \left[\frac{\rho_G U_G^2}{gD(\rho_L - \rho_G)}\right]^{1/2} = 0.35 \text{ to } 0.45. \qquad [15]$$

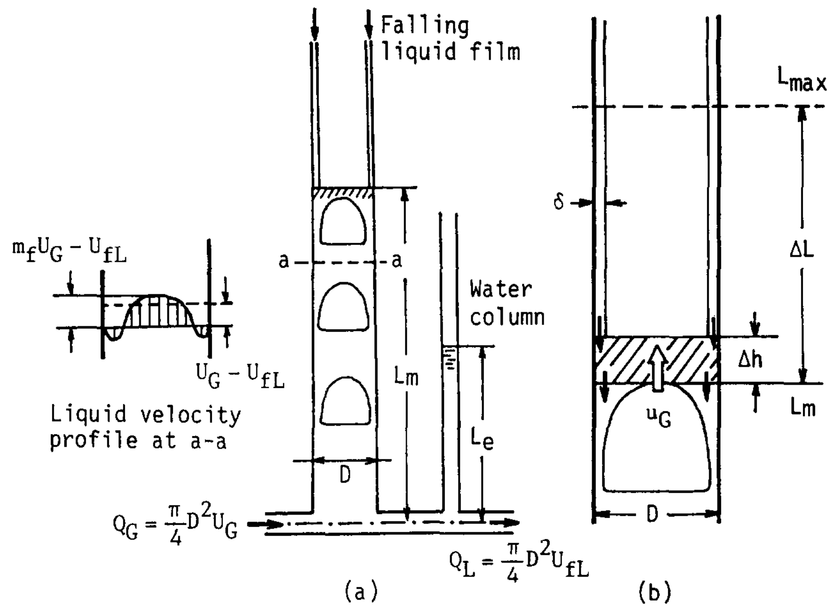

Figure 9. Two-phase mixture level swell and mixture level fluctuation by a bubbling water column with a falling film.

4.2. Level swell of the two-phase mixture in the countercurrent flow liquid column bubbling

(1) Description of the physical model. A flow state in the countercurrent flow liquid column bubbling is shown schematically in figure 9(a). The same amount of water as the falling film flow rate is drained from the bottom of the pipe and the water column height L_e is maintained at a constant value. Supposing that the flow pattern of the two-phase mixture in the lower portion of the pipe is of slug type, the mean velocity of the water between the air plugs is $U_G - U_{fL}$. Assuming the water velocity in the center portion of the pipe is $m_f U_G - U_{fL}$ and the air plug has a relative velocity to this water velocity, the rise velocity of the air plug can be expressed as

$$u_G = m_f U_G - U_{fL} + c_s\sqrt{gD}. \qquad [16]$$

Therefore, the void fraction of the mixture and the mean height of the mixture level are expressed in the same way as in [4] and [5], as follows:

$$\epsilon = \frac{U_G}{u_G} = \frac{1}{m_f + \dfrac{c_s\sqrt{gD} - U_{fL}}{U_G}} \qquad [17]$$

and

$$\frac{L_m}{L_e} = \frac{m_f U_G + c_s\sqrt{gD} - U_{fL}}{(m_f - 1)U_G + c_s\sqrt{gD} - U_{fL}}. \qquad [18]$$

In the countercurrent flow system, where the gas plugs flow upwards, the cross-sectional velocity profile in the liquid slug is considered to take a form with a convex portion in the core, such as shown in figure 9(a), even in the case of the mean water velocity $(U_G - U_{fL}) \leqslant 0$. From this consideration, the expression of [16] is used in which $m_f U_G - U_{fL}$ is applied for the water velocity in the core instead of $m_f(U_G - U_{fL})$.

In the same way as in the preceding section, it is assumed that the length of the liquid slug is within $h_L \pm \Delta h$, the mixture level height reaches L_m when the slug length is h_L and reaches L_{max} when the slug length is $h_L + \Delta h$. The state when the top of the air plug, which was associated with a liquid slug of $h_L + \Delta h$ on it, has just reached the elevation L_m is illustrated in figure 9(b). There, the liquid slug of thickness Δh is still left on the air plug. The liquid slug rises up with a decrease in its volume and reaches L_{max} after Δt_0 to disappear ($\Delta h = 0$). The mass balance for the liquid slug during this period is given by

$$\frac{\pi}{4}D^2\,\Delta h - \frac{\pi}{4}D^2\epsilon_{pm}c_s\sqrt{gD}\,\Delta t_0 + \frac{\pi}{4}D^2U_{fL}\,\Delta t_0 + \pi D\delta(\Delta L - \Delta h) = 0. \qquad [19]$$

The third term on the left-hand side of the above equation represents the water supply due to the falling film flow, and the fourth term is the amount of water which exists as the falling film in the interval $(\Delta L - \Delta h)$.

The rise height of the top of the air plug during this period is

$$\Delta L = u_G\,\Delta t_0 = (m_f U_G - U_{fL} + c_s\sqrt{gD})\,\Delta t_0. \qquad [20]$$

Substituting the above equation into [19] and considering $\Delta L \gg \Delta h$, then

$$\Delta t_0 = \frac{\Delta h}{\epsilon_{pm}c_s\sqrt{gD} - U_{fL} - \frac{4\delta}{D}(m_f U_G - U_{fL} + c_s\sqrt{gD})}. \qquad [21]$$

Therefore,

$$\frac{\Delta L}{L_e} = \frac{\Delta h}{L_e}\cdot\frac{m_f}{\epsilon_{pm}} \times \frac{U_G + \dfrac{c_s\sqrt{gD} - U_{fL}}{m_f}}{c_s\sqrt{gD} - \dfrac{U_{fL}}{\epsilon_{pm}} - \dfrac{4\delta}{\epsilon_{pm}D}(m_f U_G + c_s\sqrt{gD} - U_{fL})}. \qquad [22]$$

Considering that m_f and ϵ_{pm} have values close to 1 and $4\delta/D \ll 1$, the above equation can be approximated as follows:

$$\frac{\Delta L}{L_e} = N_f\frac{U_G + c_s\sqrt{gD} - U_{fL}}{c_s\sqrt{gD} - U_{fL} - \frac{4\delta}{D}(U_G + c_s\sqrt{gD} - U_{fL})}, \qquad [23]$$

where

$$N_f = \frac{\Delta h}{L_e}\cdot\frac{m_f}{\epsilon_{pm}}.$$

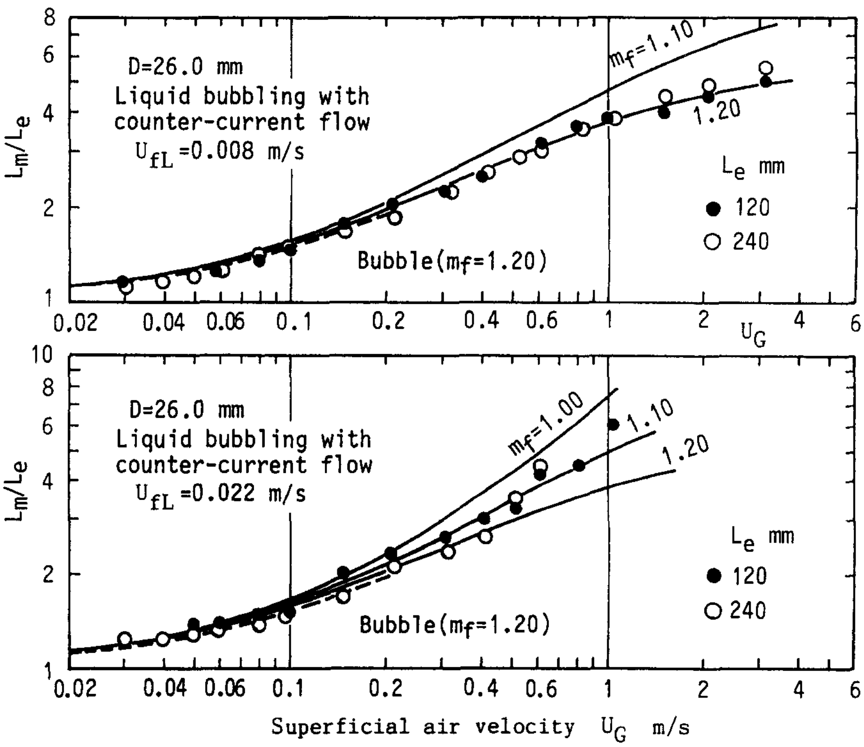

Figure 10. Mean height of the two-phase mixture level (countercurrent flow liquid column bubbling).

The falling film thickness δ can be predicted from the falling film flow rate per unit periphery (Ueda & Tanaka 1974). In the present calculation, the thickness was obtained with Kapitza's equation, introduced in the paper by Fulford (1964), and universal velocity profile equations. These equations are presented briefly in the appendix.

(2) Comparison with the experimental results. Experimental results for L_m/L_e are compared with the values calculated with [18] in figures 3 and 10. The solid lines in these figures show the values obtained for $m_f = 1.0$, 1.1 and 1.2, respectively. The calculated results reproduce well a trend of the experimental results in the slug flow region.

Since the falling water film brings a considerable amount of momentum into the liquid slug, it is considered that the falling film has an effect on the shape and rise velocity of the air plug. As shown in figure 10, the rise velocity of the air plug tends to decrease and then L_m/L_e tends to increase as the falling film flow rate is increased.

The values of m_f are approx. 1.15–1.2 in a range of lower superficial velocities U_{fL}. The values are the same as those in the stagnant liquid column bubbling. However, m_f decreases with an increase in U_{fL}, and also with a decrease in L_e, as shown in figures 3 and 10.

Comparing the calculated results with the experimental data, an appropriate value of m_f was found for each experimental condition. The values thus derived are presented in figure 11. Although the results are somewhat scattered, the value of m_f can be correlated as follows:

$$m_f = (1.175 \pm 0.075) - 1.15\frac{U_{fL}}{c_s\sqrt{gD}}\left(\frac{D}{L_e}\right)^{1/2}. \qquad [24]$$

The value of L_m/L_e for the bubbly flow region can be calculated with [18] by using [11] in place of $c_s(gD)^{1/2}$. The values calculated by $m_f = 1.20$ are in good agreement with the experimental results.

Experimental results for the fluctuation amplitude of the mixture level are compared with the values calculated with [23] in figures 3 and 12. The calculated results reproduce well a trend of the experimental data in the slug flow region. The experimental results are close to the values calculated with $N_f = 0.10$ on average and range within the values obtained with

$$N_f = 0.08 \text{ to } 0.15. \qquad [25]$$

The values of N_f are a little smaller than the values of N for the stagnant liquid column bubbling. It seems that the length of the liquid slug is equalized by the inflow of the falling liquid film.

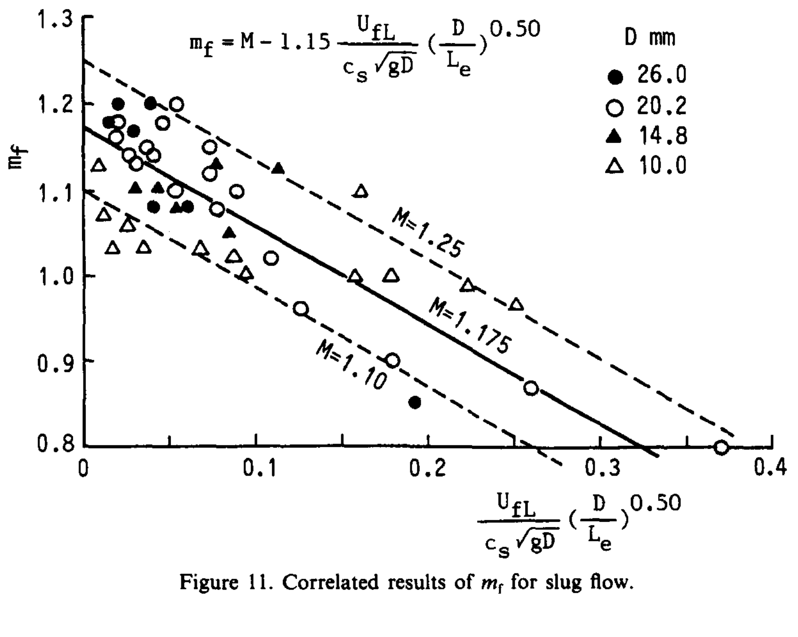

Figure 11. Correlated results of m_f for slug flow.

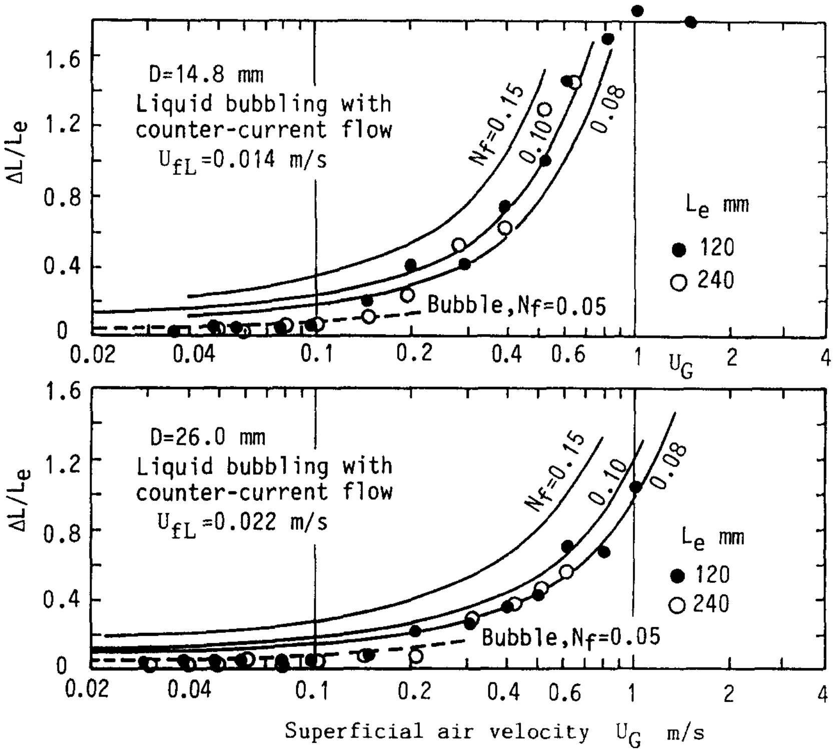

Figure 12. Fluctuation amplitude of the two-phase mixture level (countercurrent flow liquid column bubbling).

Although $\Delta L/L_e$ in the bubbly flow region is small, the experimental results agree pretty well with the values calculated with [23] by using [11] instead of $c_s(gD)^{1/2}$ and

$$N_f = 0.05, \tag{25'}$$

as in the stagnant liquid column bubbling.

The region where L_m/L_e and $\Delta L/L_e$ show bubbly-type characteristics is a little wider than that in the stagnant liquid column bubbling. The transition of the characteristics from bubbly to slug type occurs in the range of

$$\epsilon = 0.40 \text{ to } 0.48 \quad (L_m/L_e = 1.7 \text{ to } 1.9). \tag{26}$$

5. CONCLUSIONS

The two-phase mixture level swell in vertical pipes was investigated for both stagnant liquid column bubbling and countercurrent flow liquid column bubbling. The conclusions derived are as follows:

(1) At low flow rates of injected air, the flow pattern is of bubbly type and the two-phase mixture level swell and the level fluctuation amplitude are small. However, as the flow rate of the injected air is increased and the flow pattern changes to a slug type, both the level swell and the level fluctuation amplitude increase sharply.

(2) The mean height of the two-phase mixture level and the level fluctuation amplitude in the countercurrent flow liquid column bubbling are larger than those in the stagnant liquid column bubbling. The differences increase as the flow rate of the falling film is increased.

(3) Relations between the flow rate(s) of the injected air (and the falling film) and the mean height of the two-phase mixture level and the level fluctuation amplitude are analyzed physically. Comparing the results with the experimental data for stagnant liquid column bubbling and bubbling with a falling film, the

correlations to predict the above relations are proposed. The correlations reproduce the experimental results well.

REFERENCES

AKAGAWA, K., HAMAGUCHI, H. & SAKAGUCHI, T. 1970 Study on differential pressure fluctuation of two-phase slug flow (third report). *Trans. JSME* **36,** 1535–1542.

CUNNINGHAM, J. P. & YEH, H. C. 1973 Experiments and void correlation for PWR small-break LOCA conditions. *Trans. Am. Nucl. Soc.* **17,** 369–370.

FULFORD, G. D. 1964 The flow of liquid in thin films. *Adv. Chem. Engng* **5,** 151–236.

GRIFFITH, P. & WALLIS, G. B. 1961 Two-phase slug flow. *Trans. ASME Ser.* **C83,** 307–320.

NICKLIN, D. J., WILKES, J. O. & DAVIDSON, J. F. 1962 Two-phase flow in vertical flow. *Trans. Inst. Chem. Engrs* **40,** 61–68.

PEEBLES, F. N. & GARBER, H. J. 1953 Studies on the motion of gas bubbles in liquid. *Chem. Engng Prog.* **49,** 88–97.

UEDA, T. 1981 *Gas–Liquid Two-phase Flow*, pp. 108–109. Yokendo Co., Tokyo.

UEDA, T. & MIYASHITA, T. 1990 On the performance limit of closed two-phase thermosiphons. *Trans. JSME* **B58,** 1746–1752.

UEDA, T. & TANAKA, T. 1974 Studies of liquid film flow in two-phase annular and annular-mist flow regions (Part 1, Downflow in a vertical tube). *Bull. JSME* **17,** 603–613.

WHITE, E. T. & BEARDMORE, R. H. 1962 The velocity of rise of single cylindrical air bubbles through liquids contained in vertical tubes. *Chem. Engng Sci.* **17,** 351–361.

WILSON, J. F., GRANDA, R. J. & PATTERSON, J. F. 1962 The velocity of rising steam in a bubbling two-phase mixture. *Trans. Am. Nucl. Soc.* **5,** 151–152.

APPENDIX

Mean Film Thickness of a Falling Liquid Film

The flow rate of a falling liquid film per unit periphery and the film Reynolds number are expressed as follows:

$$\Gamma = \frac{\rho_L Q_L}{\pi D}, \quad \mathrm{Re_f} = \frac{4\Gamma}{\eta_L} = \frac{\rho_L D U_{fL}}{\eta_L}.$$

It is known that the falling film thicknesses calculated with Kapitza's equation and the universal velocity profile equations agree well with measured results for laminar film flow with interfacial waves and for higher $\mathrm{Re_f}$, respectively (Ueda & Tanaka 1974). In the present study Kapitza's equation,

$$\delta\left(\frac{g\rho_L^2}{\eta_L^2}\right)^{1/3} = \left(\frac{2.4}{4}\right)^{1/3}\mathrm{Re_f^{1/3}},$$

was used to obtain the mean film thickness δ for $\mathrm{Re_f} \leqslant 500$. For $\mathrm{Re_f} > 500$, the following relations, which are derived from the universal velocity profile equations, were used:

$$\mathrm{Re_f} = 2(\delta^+)^2, \qquad \delta^+ \leqslant 5;$$

$$\mathrm{Re_f} = 50 - 32.2\delta^+ + 20\delta^+ \ln \delta^+, \qquad \delta^+ \leqslant 30;$$

and

$$\mathrm{Re_f} = -256 + 12\delta^+ + 10\delta^+ \ln \delta^+, \qquad \delta^+ > 30;$$

where

$$\delta^+ = \delta^{3/2}\left(\frac{g\rho_L^2}{\eta_L^2}\right)^{1/2}.$$